doi:10.1111/j.1558-5646.2010.01211.x

EVIDENCE OF CONSTRAINED PHENOTYPIC EVOLUTION IN A CRYPTIC SPECIES COMPLEX OF AGAMID LIZARDS

Katie L. Smith,[1,2,3] Luke J. Harmon,[4] Luke P. Shoo,[1,5] and Jane Melville[1]

[1]*Department of Sciences, Museum Victoria, Melbourne, Victoria 3001, Australia*

[2]*E-mail: kasmith@museum.vic.gov.au*

[3]*Department of Zoology, University of Melbourne, Victoria, 3010, Australia*

[4]*Department of Biological Sciences, University of Idaho, Moscow, Idaho 83844-3051*

Received June 30, 2008
Accepted November 23, 2010

Lineages that exhibit little morphological change over time provide a unique opportunity to explore whether nonadaptive or adaptive processes explain the conservation of morphology over evolutionary time scales. We provide the most comprehensive evaluation to date of the evolutionary processes leading to morphological similarity among species in a cryptic species complex, incorporating two agamid lizard species (*Diporiphora magna* and *D. bilineata*). Phylogenetic analysis of mitochondrial (ND2) and nuclear (RAG-1) gene regions revealed the existence of eight deeply divergent clades. Analysis of morphological data confirmed the presence of cryptic species among these clades. Alternative evolutionary hypotheses for the morphological similarity of species were tested using a combination of phylogenetic, morphological, and ecological data. Likelihood model testing of morphological data suggested a history of constrained phenotypic evolution where lineages have a tendency to return to their medial state, whereas ecological data showed support for both Brownian motion and constrained evolution. Thus, there was an overriding signature of constrained evolution influencing morphological divergence between clades. Our study illustrates the utility of using a combination of phylogenetic, morphological, and ecological data to investigate evolutionary mechanisms maintaining cryptic species.

KEY WORDS: **Agamidae, morphological evolution, morphological stasis, nonadaptive, phylogenetics.**

An essential component of evolutionary biology research is to evaluate the relative contribution of different evolutionary processes involved in producing contemporary patterns of morphological diversity (Lee 2000; Lemos et al. 2001). Research has commonly focused on the evolutionary processes contributing to high levels of morphological diversity among species, as seen in adaptive radiations (e.g., Warheit et al. 1999; Losos and Miles 2002; Glor et al. 2004). However, the increasing use of molecular phylogenetic techniques has highlighted the prevalence of genetically divergent populations that exhibit very little morphological change through time (Knowlton 1993; Kozak et al. 2006). Known as cryptic species, these morphologically similar organisms often have long independent evolutionary histories, providing an opportunity to investigate the ecological and evolutionary mechanisms that have led to their morphological conservatism (Larson 1989; Milinkovitch 1995).

Cryptic species occur when daughter species accumulate genetic differences without apparent morphological divergence (Avise et al. 1987; Bickford et al. 2006; Mathews et al. 2002). Cryptic species highlight the complexities of phenotypic evolution (Bruna et al. 1996) as morphological similarities can be attributed to both adaptive and nonadaptive evolution (Schluter 2000). Even if neutral genetic divergence between

[5]Current address: School of Biological Sciences, The University of Queensland, St. Lucia, QLD 4072, Australia.

species is attributable to drift, the morphological conservatism of the species could in theory result from niche conservatism (Wiens 2004; Wiens and Graham 2005) and stabilizing selection (Eldredge and Gould 1972; Charlesworth et al. 1982; Futuyma 1998). In this case, adaptive processes, where species are adapted to their environment through natural selection, would be involved in the evolution of these cryptic species. Consequently, it is fundamentally important to address patterns of morphological and genetic change in association with environment in cryptic species complexes.

There are three processes that could, in theory, lead to the evolution of phenotypic conservatism in historically isolated lineages: neutral genetic drift, constrained evolution, and correlated evolution. Each of these processes display clearly definable evolutionary patterns. First, when adaptive scenarios are not supported, the nature of genetic evolution implies that morphological similarity among evolutionary lineages may be primarily shaped by neutral, nonadaptive processes, where chance events determine which alleles will be carried forward while others disappear (Bostwick and Brady 2002). As such, cryptic species maintained by neutral genetic drift are characterized by phylogenetic and phenotypic differences that accumulate proportionally through time (Lynch 1990). On the other hand, constrained evolution may lead to morphological conservatism and can result from a number of processes. For example, lineages may exhibit long-term morphological stasis due to the effects of stabilizing selection (e.g., Charlesworth et al 1982; Schneider and Moritz 1999; Wiens and Graham 2005) or developmental constraints (e.g., Wake 1983, 1991; Maynard Smith et al. 1985). By selecting against extreme phenotypic characters, stabilizing selection prevents divergence of form and function, and distinct populations will remain similar over long periods of time. Additionally, morphological conservatism may also result from constraints on intrinsic developmental features by imposing bounds on phenotypic variation (Maynard Smith et al. 1985; Wake 1991).

Finally, correlated evolution may drive morphological similarity in cryptic species complexes. Multiple evolutionary origins of morphological traits associated with similar ecological occupation suggest that particular habitats elicit comparable adaptive evolutionary responses (Schluter and McPhail 1993; Glor et al. 2003; Harmon et al. 2005). As a result, lineages within a cryptic radiation may have developed morphological traits that are adaptations for a particular selective regime (Pfenninger et al. 2003), such that morphology is strongly correlated with habitat use, but not with phylogeny (Harvey and Pagel 1991; Wainwright and Reilly 1994).

Despite the widespread discovery of cryptic species complexes in phylogenetic studies, research has not focused on testing alternative hypotheses of the evolutionary processes leading to variation in form and function among cryptic species and our understanding of these processes remains poor. Due to this lack of research, evolutionary neutrality, which could be considered a null model, has not been rejected as the most parsimonious explanation. Molecular phylogenetics, combined with macroevolutionary models, allow us to explicitly test hypotheses of the tempo and mode of species diversification (Harmon et al. 2003). However, most of these recently developed analytical methods have been applied to investigating evolutionary processes in adaptive radiations, where clades exhibit rapid divergence into a variety of adaptive morphologies (e.g., Schluter 2000; Losos and Miles 2002). Very few studies have quantified the tempo and mode of diversification among clades that contain very low levels of phenotypic disparity (but see Kozak et al. 2005; Adams et al. 2009). Incorporation of these techniques allows new insight into evolutionary processes that may lead to a decoupling of genetic and morphological diversity.

The sympatric lizard species, *Diporiphora magna* and *D. bilineata*, are ideal candidates to study the evolutionary processes underlying the maintenance of morphological stasis in cryptic species. *Diporiphora magna* and *D. bilineata* show a high degree of morphological similarity throughout their ranges (Greer 1989), which has led to taxonomic confusion in attempts to identify these species. Presently, identification has been limited to morphological comparisons among a small subset of individuals, leading to numerous taxonomic keys being developed that are based on variable characters, such as body size, patterning, and coloration (Storr 1974; Wilson and Knowles 1988; Cogger 2000). Both species are a prominent component of the reptile fauna of the savannah woodlands of tropical northern Australia, with overlapping distributions that form a near continuous range across northern regions (Fig. 1).

In this article, we demonstrate using phylogenetic analyses that the two recognized species are actually comprised of multiple deeply divergent clades. The taxonomic confusion that surrounds identification of these species suggested these recovered clades would also represent cryptic species. We aimed to quantify morphological conservatism among these deeply divergent clades and investigate the processes maintaining this conservatism. We undertook the first detailed study of *D. magna* and *D. bilineata*, incorporating phylogeographic, morphological, and ecological data to investigate the evolutionary processes governing phenotypic variation in these morphologically similar but genetically distinct lineages.

Methods

HYPOTHESES

We tested three hypotheses using comparative evolutionary methods to assess the extent to which phenotypic patterns can be

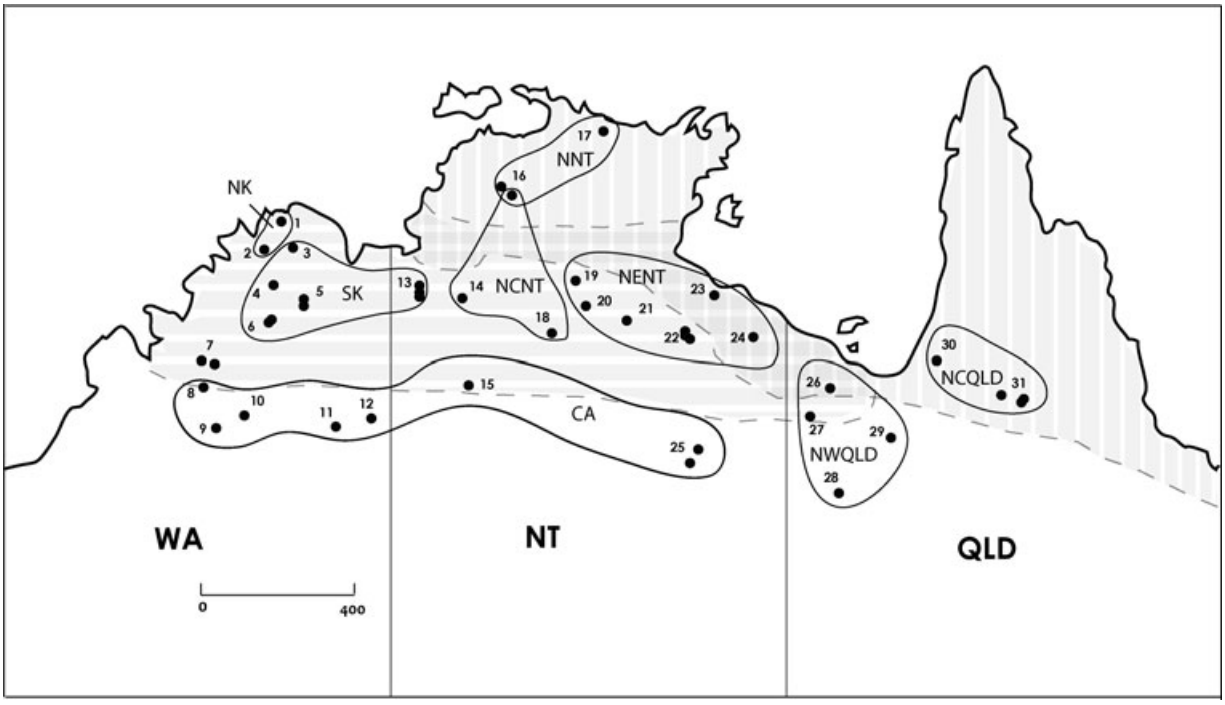

Figure 1. Map of northern Australia showing collecting localities and clade distribution for the lineages of the *D. magna-D. bilineata* complex identified in this study. Numbers indicate a sampled population (details provided Appendix S1) and clades are labeled according to geographic location. Currently described distributions of *D. magna* (horizontal shading) and *D. bilineata* (vertical shading) are enclosed within gray dashed lines, as adapted from Cogger (2000). WA = Western Australia, NT = Northern Territory, QLD = Queensland.

attributed to nonadaptive change, constrained evolution, and correlated evolution.

(1) Phenotypic evolution fits a neutral model of Brownian motion for both morphology and ecology.
(2) Phenotypic evolution fits a model of constrained evolution for both morphology and ecology.
(3) Phenotypic evolution fits a model of correlated evolution, where there is a correlation between morphology and ecology.

We note that hypothesis (3) is potentially compatible with either (1) or (2), because both neutral and constrained models of evolution can lead to correlations between morphology and ecology. Details of the comparative evolutionary methods used to explore each of these hypotheses are described below.

PHYLOGENETIC ANALYSIS

DNA extraction and sequencing

Ethanol-preserved tissue samples were obtained for DNA sequencing from field-caught lizards (collected between 2003 and 2006) and museum specimens of *D. magna* and *D. bilineata* from throughout their currently described distribution (Fig. 1, locality details are in Appendix S1). Seven of the 14 other species recognized within the *Diporiphora* genus (*D. winneckei*, *D. pindan*, *D. valens*, *D. lalliae*, *D. albilabris*, *D. bennetti*, and *D. superba*) were also sequenced in this study to determine the phylogenetic placement of the study species within the genus. Additionally, we included two previously published sequences of *D. bilineata* and *D. magna* in our analysis (Schulte et al. 2003). Sequences from *Amphibolurus muricatus* and *Tympanocryptis lineata* were used as outgroups (Appendix S1).

We sequenced a region of mtDNA (~1400 bp), incorporating the entire protein-coding region ND2 (NADH dehydrogenase subunit two), five tRNAs ($tRNA^{Trp}$, $tRNA^{Ala}$, $tRNA^{Asn}$, $tRNA^{Cys}$, $tRNA^{Tyr}$), O_L (origin of light-strand synthesis) to the beginning of the protein-coding gene COI (subunit I of cytochrome c oxidase), according to protocols previously used in Australian agamids (Melville et al. 2001; Schulte et al. 2003). In addition, we sequenced ~1000 bp of a nuclear gene (recombination activating gene-1 exon [RAG-1]).

We isolated whole genomic DNA using a Proteinase K digestion and chloroform-isoamyl alcohol extraction protocol (Shoo et al. 2008). Three primers were used for amplification and sequencing of ND2 (H4419 [Macey et al. 2000], H5934a [Macey et al. 1997] and COIr.aga [Shoo et al. 2008]) and two for RAG-1 (JRAG.f and JRAG.r [Shoo et al. 2008]). Sequences were initially aligned by eye, and amino acid translations were then used to align protein-coding regions, and secondary structure models

were used to align tRNAs (Macey et al. 1997). Unalignable regions were excluded from phylogenetic analyses.

Phylogenetic relationships

We constructed three phylogenetic trees: mitochondrial (ND2), nuclear (RAG-1), and combined (ND2 + RAG-1). The mitochondrial dataset included 102 new sequences of *Diporiphora* and five previously published sequences for the ND2 region (Appendix S1). The nuclear dataset consisted of a subset of these samples, incorporating 43 new sequences and two previously published sequences for the RAG-1 region (Appendix S1). The combined dataset included these RAG-1 sequences and the corresponding mitochondrial sequences from the same individuals.

We analyzed the mitochondrial and nuclear datasets using partitioned Bayesian analyses (see Nylander et al. 2004) in MrBayes version 3.1. (Ronquist et al. 2005). We conducted separate analyses using the mitochondrial dataset only, the nuclear dataset only, and a combined dataset of the mitochondrial and nuclear regions. It was important to conduct separate analyses for each of the gene regions to compare differences in the topology of each phylogeny. As different gene regions can have different evolutionary histories, this allowed us to evaluate each cryptic lineage for the mitochondrial and nuclear DNA datasets separately. A partition homogeneity test (PHT) was used to test for congruence between the nuclear and mitochondrial datasets (Farris et al. 1994). In the PHT, heuristic searches were performed with simple taxon addition and TBR branch swapping, and replicated 100 times using PAUP* version 4.0 (Swofford 2002). Global congruence tests such as these may not be accurate for assessing large datasets due to potential localized differences in the histories of each datasets. Therefore, we also assessed support using a method that compares support for conflicting clades between datasets (Wiens 1998). The concatenated dataset was subsequently used in further evolutionary analyses, as there was low heterogeneity between each of the separate ND2 and RAG-1 analyses. In particular, both trees showed high branch support for each of the recovered lineages and each of the lineages had long branches leading to each of the clades, implying these lineages do not result from a recent speciation event. Thus, these trees did not show qualities of gene trees that were likely to mislead inference of species relationships when concatenated (Edwards et al. 2007), and the concatenated tree was therefore used in further analyses. In addition, we created an ultrametric tree from the consensus tree of the posterior distribution of the combined dataset using penalized likelihood (Sanderson 2002; smoothing parameter = 6.9, determined by cross-validation; root age arbitrarily set to 1000). All comparative analyses below used the resulting ultrametric tree.

To account for the possibility of different evolutionary rates and parameters between gene regions, we assessed support for alternative data partitioning schemes, which used alternative models based on genes and codon positions in coding regions (Brandley et al. 2005; Appendix S2). We selected a model of sequence evolution based on the Akaike information criterion (AIC) for each partition, as implemented in the program ModelTest version 3.06 (Posada and Crandall 1998). All optimal models of evolution for each partitioning scheme are available in Appendix S2. All Bayesian analyses were initiated from random starting trees and run for 5,000,000 generations using four incrementally heated Markov chains that were sampled every 100 generations. The optimal models of evolution were enforced for each gene region and model parameters were unlinked. Standard deviation of split frequencies was used as a convergence diagnostic to confirm suitability of run length. For all analyses, we used potential scale reduction factor (PSRF) values that were close to 1.0, indicating that a good sample of the posterior probability distribution had been achieved. The plot of log-likelihood values and generation number was then used to provide evidence that the analysis had reached stationarity and to determine appropriate "burn-in" for discarding initial samples. We compared the fit of each of the partitioning schemes using Bayes factors, estimated using the *sump* command in MrBayes (Kass and Raftery 1995; Brandley et al. 2005). We then selected the simplest partitioning scheme that was supported over other models by 2 ln Bayes factors greater than 10 (Kass and Raftery 1995). We generated 50% majority rule consensus trees with posterior probabilities for branch support (Ronquist et al. 2005). This analysis assumes no recombination of RAG-1, therefore, prior to phylogenetic analysis, we conducted a recombination test for RAG-1. We tested for recombination using a Bayesian multiple change point model, *DualBrothers* (Suchard et al. 2003; Minin et al. 2005), implemented in the software package *Geneious* (Biomatters; Drummond et al. 2009). We used the default parameters including Markov chain Monte Carlo (MCMC) chain length of 1,000,000 generations. As we found no significant evidence of recombination (see below), the nuclear dataset of RAG-1 was deemed relevant for phylogenetic analyses.

MORPHOLOGICAL DATA

We used morphological data to test for the presence of cryptic species among the recovered phylogenetic lineages. We collected data on nine morphological measurements and 25 meristic character counts from adult field-caught and museum voucher specimens (locality details provided in Appendix S3). Measurements were taken from areas of the body that have been shown to be of adaptive and ecological importance in morphological studies of iguanian species, including the Agamidae (Bickel and Losos 2002; Schulte et al. 2004; Melville et al. 2006). Only adults (>35 mm snout-to-vent length [Wilson and Knowles 1988]) were used in analyses to avoid possible confounding influence of ontogenetic changes in morphological proportions. All morphological measurements showed significant sexual dimorphism, which is

a common trait across lizards (Appendix S4; reviewed in Losos et al. 2003). As such, males and females were analyzed separately (males: $N = 56$; females: $N = 37$; across eight populations with ≥ 5 individuals/population). Measurements included snout-vent length (SVL), tail length, head length, head width, hindlimb length, forelimb length, interlimb length, metacarpal length, and metatarsal length (Appendix S5).

All morphological measurement variables were log-transformed prior to analyses. The allometric effects of body size were removed by calculating the residuals of each variable regressed against SVL. A principal components analysis (PCA) was used to extract independent morphological axes of body shape variation from log-transformed SVL and size-independent variables. We analyzed the meristic characters using correspondence analysis, which converted the raw data into a set of continuously varying multivariate axes (Legendre and Legendre 1998). To adjust for body size differences, the two meristic characters that were continuous (tympanum size and blotch diameter) were regressed against SVL and the residuals were used in subsequent analyses.

ECOLOGICAL MEASUREMENTS

We collected habitat-use data for field-captured lizards ($N = 71$). In total, 23 ecological variables were collected describing the thermal and microhabitat characteristics within a 3 m radius surrounding the point at which the captured lizards were first observed (details provided in Appendix S6). Body temperature was measured immediately upon capture using an Omega^{TM} portable digital thermometer with thermistor probe. Ecological variables were subsequently separated into two categories for analysis to allow an unambiguous interpretation of the data. These two categories were microhabitat occupation variables, which were dependent on the behavior of the lizard (including perch description, closest shelter, and closest vegetation); and structural ecology variables, which were related to the general ecological features in the area (including descriptions of substrate type and ground, shrub, and tree vegetation).

A PCA was used to reduce the ecological variables into a smaller number of components for further analyses. Categorical measurements of perch (trunk, termite mound, stick, log) and shelter type (rock, grass, trunk) were analyzed separately. Prior to analyses, percentage variables were arcsine transformed and the remaining variables were log transformed to ensure normality.

In addition to these microhabitat data, broad-scale environmental data were analyzed to provide an understanding of ecological differences between clades related to their distribution. Spatial climate layers were derived for each sampled lizard using the Anuclim 5.1 software (McMahon et al. 1995) and a 250-m resolution Digital Elevation Model (created from GEODATA 9 Second DEM Version 2; Geoscience Australia, http://www.ga.gov.au/; McMahon et al. 1995). Six parameters that were deemed to play an important role in the distribution of Australian reptile species were selected for further analysis (e.g., Woinarski et al. 1999; Kearney et al. 2003). These were annual mean temperature, maximum temperature of warmest period, minimum temperature of coldest period, annual precipitation, annual mean radiation, and annual mean moisture index. A PCA was used to reduce the variables to a smaller number of components for further analyses.

DIFFERENCES AMONG MAJOR CLADES IN MORPHOLOGY AND HABITAT USE

Our combined phylogenetic tree revealed eight well-supported monophyletic lineages within the species complex (see below). We used discriminant function analysis to test for the presence of cryptic species, by assessing whether each of the recovered phylogenetic lineages could be separated based on phenotypic size and shape variables. We conducted analyses using (1) morphological measurements and meristic characters combined, and (2) meristic characters alone. Analyses were conducted separately for males and females. Furthermore, to assess whether these eight lineages can be considered morphologically similar in relation to other closely related species in the genus, we conducted an analogous discriminant function analysis on 10 previously described *Diporiphora* species. These species were selected as they are phylogenetically closely related to *D. bilineata* and *D. magna*, according to a previously published phylogeny (Schulte et al. 2003). We measured up to five museum specimens from each species as described above for the cryptic lineages (Appendix S3).

In addition, to visualize differences in morphology and ecology, individuals were grouped according to phylogenetic clades and mean PC scores and singular scores (CA) were plotted in Euclidian space. We performed univariate analyses of variance (ANOVAs) on PC scores and singular scores to test for differences among these clades in morphology and habitat use (Legendre and Legendre 1998). We used Bonferroni sequential adjustments to estimate significance levels (Rice 1989).

TESTING EVOLUTIONARY HYPOTHESES

Phenotypic evolution fits a neutral model of Brownian motion

We examined the extent of phylogenetic structure in morphological and ecological diversity. A statistical test of phylogenetic signal was used to assess whether there is a tendency for related species to resemble each other (Blomberg et al. 2003). A significant result would suggest that phenotypic evolution among clades is related to their phylogeny. Alternatively, a nonsignificant result would suggest that historical signal had been overwritten by nonrandom processes (e.g., natural selection; Revell et al. 2008). However, it is important to note that support for Brownian motion may also provide evidence of an evolutionary process that tracks

randomly shifting adaptive peaks through time (Lynch 1990). We evaluated phylogenetic signal in both morphological and ecological axes using the K-statistic, which indicates the amount of phylogenetic signal relative to Brownian motion character evolution (Blomberg et al. 2003). For the single main axis of variation in each dataset (PC1 or CA1), we calculated K and an associated *P*-value for this test statistic using the randomization procedure described in Blomberg et al. (2003), as implemented in r code (Kembell et al. 2009). Small *P*-values indicate significant support for phylogenetic structure in the dataset.

Phenotypic evolution fits a model of constrained evolution

We compared fits of four global models to the data from all eight clades using AIC (Akaike 1974) in r statistical software using the GEIGER package (Harmon et al. 2008): (1) BM: a single rate random walk (modeled as Brownian motion, two parameters: θ, the starting character state, and σ^2, the rate of diffusion); (2) EB: a random walk model in which the rate parameter decreases through time (modeled as early burst, equivalent to the ACDC model in Blomberg et al. 2003, three parameters, θ, the starting character state, σ^2, the rate of diffusion at the beginning of the simulation, and a, the decay constant that specifies how the rate of evolution slows through time); and two constrained random walk models, such that species have a tendency to return to a medial value, which consisted of (3) OU: modeled as an Ornstein–Uhlenbeck process (three parameters, θ, the medial value for the trait, σ^2, the rate of diffusion, and α, the strength of the pull toward the medial value; Butler and King 2004); and (4) WN: modeled as white noise (two parameters, θ, the mean value for the trait, and σ^2, the variance across tip species; Hunt 2006). The single rate model describes the evolution of a continuous character undergoing a random walk through time, whereas the early burst model describes a situation similar to an adaptive radiation, where there is elevated variance in morphology early in the tree, but is lowered in recent times.

Models (3) and (4) are the most relevant to our hypothesis because they represent the patterns expected when trait evolution is constrained through time (see Harmon et al. 2010). The WN model has not previously been used in this context, however it describes a situation in which characters are drawn from the same normal distribution regardless of their evolutionary relationships. One way to get this pattern is the presence of very strong constrained evolution; WN is the limiting case of an OU model with an infinitely strong constraint parameter. Both the WN and the Ornstein–Uhlenbeck constant constraint model (OU) predict that variance in body size among species will be weakly related or even unrelated to clade age. This is because under these models, young clades will show similar amounts of variance in body size as the whole clade, a pattern characteristic of constrained evolution (Hansen 1997; Butler and King 2004). We calculated AIC values for the main axis of variation (PC1 or CA1) in all 10 datasets, separating the sexes. A lower AIC value indicates the model provides a better fit for that dataset (Burnham and Anderson 2002).

We calculated disparity-through-time plots to examine the time course of morphological diversification (Harmon et al. 2003). Disparity was calculated from average pairwise Euclidean distances between species, for morphological and ecological characters, obtained from all axes of the principal components and correspondence analyses above. Using the combined Bayesian phylogeny, we calculated disparity for the entire clade and then for each subclade defined by a node in that phylogeny. We then calculated the average subclade disparity across clades at various time slices through the phylogenetic tree, following the methods described in Harmon et al. (2003). All clades whose stem branch crosses a given time slice are included in the average disparity calculation for that interval; thus, this value can be thought of as an average of the disparity of all clades of a given age relative to the disparity of the clade as a whole.

To calculate how much mean disparity differed from that under a null hypothesis of character evolution, we compared these disparity values to those obtained through simulations of traits evolving under a multivariate Brownian motion model (Harmon et al. 2003). For these simulations, a rate matrix describing the dynamics of the multivariate Brownian motion model is needed; we used the mean sum of squares and cross-products matrix of independent contrasts, which provides an unbiased estimate of the evolutionary rate matrix for each dataset (Revell and Harmon 2008). A 95% confidence interval was also calculated, which together with the median simulated DDT value can be used to statistically examine when in time the observed disparity is significantly greater or less than expected under a particular model of evolution.

The resulting disparity-through-time graphs provide a visual display of how patterns of within-clade disparity vary across different levels in the phylogenetic tree. When the data are below the Brownian expectation, it suggests that the species within clades of that age range are not as diverse as expected, and that most of the variation in traits is among, rather than within, clades. This might correspond to a model in which clades exhibit rapid evolution just after they originate, followed by relative stasis (as in the EB model, above). On the other hand, if the data are above the Brownian model, then it suggests the species within clades are more diverse than expected and would therefore be overlapping in diversity with other clades at that time period. This can result, for example, when evolutionary change occurs within bounds (as in the OU and WN models, above) or when the rate of change has accelerated toward the present day (see Appendix in Harmon et al. 2003 for further details).

Phenotypic evolution fits a model of correlated evolution

We used partial Mantel analyses (Mantel 1967; Smouse 1986) to test whether there was a significant evolutionary correlation between morphology and ecology. This method was used to examine the correlation between morphology and ecology, while simultaneously accounting for phylogenetic effects. A significant correlation between morphology and ecology, after controlling for the effects of phylogenetic relatedness, would support the hypothesis that morphological differences between clades results from adaptation to different habitat occupation. There are various limitations to using partial Mantel tests, including poor statistical performance compared to other analyses, low power, and high type-I error in some cases (Raufaste and Rousset 2001; Castellano and Balleto 2002; Harmon and Glor 2010). However, we know of no alternative phylogenetic multivariate analysis for the hypotheses tested here.

Only lizards that had data for all variables were included in each Mantel test and all analyses were performed separately on each sex (Males: $N = 25$–39; Females: $N = 18$–23; Appendix S15). Partial Mantel tests were conducted using the PASSAGE software (Rosenberg 2002), testing the correlation between various dissimilarity matrices: (1) morphological measurements; (2) meristic characters; (3) microhabitat occupation; (4) structural ecology; (5) environment; and (6) phylogenetic distance. Euclidian distance matrices (matrix 1, 2, 3, 4, and 5) were compiled in SYSTAT 10.2 using the clade means calculated from the PC or CA scores for each individual lizard in respective multidimensional space. For microhabitat occupation, structural ecology, and environment matrices, we calculated distances in the coordinate space defined by the first two (environment) or four (microhabitat and structural ecology) PC axes together, which allowed a better estimate of overall habitat use differences among species. Each of the PC axes and CA dimensions for morphological measurements and meristic characters were complied into separate matrices. The matrix of phylogenetic relationships was created from the maximum likelihood analysis with TreeEdit V1.0a4-61 (Rambaut and Charleston 2000) using patristic distances of branch lengths separating the individuals. We used Bonferroni correction for multiple tests within each data category for an overall 5% confidence level ($\alpha = 0.05$).

Results

PHYLOGEOGRAPHIC RELATIONSHIPS

We conducted separate analyses of the mtDNA (Appendix S7), nuclear (Appendix S8), and concatenated datasets (Fig. 2). For the mitochondrial dataset, 93 new mtDNA sequences of the *D. magna* and *D. bilineata* complex, incorporating 1279 bp, were analyzed. An additional seven sequences from individuals morphologically identified as *D. lalliae* were included in the analyses, as they were found to fall within the *D. magna-D. bilineata* clade. These 100 sequences were aligned with 10 mtDNA sequences from other *Diporiphora* species (*D. albilabris, D. bennetti, D. winneckei* [four individuals], *D. superba, D. pindan, D. lalliae,* and *D. valens*) for phylogenetic analysis. Single sequences from *A. muricatus* and *T. lineata* were included as outgroups. All base positions in the protein-coding gene ND2 were alignable. Selected loop regions of tRNA genes, COI, and noncoding regions between genes were unalignable and excluded from analysis. Of the 1279 unambiguous sites, 661 were variable and 549 parsimony informative.

For the mitochondrial dataset, a 50% majority-rules tree recovered from the partitioned analysis (Appendix S7) revealed eight well-supported and highly divergent clades within the *D. magna* and *D. bilineata* complex (Bayesian posterior probabilities = 1.00). These eight lineages are characterized by deep interclade divergences (uncorrected pairwise distance: 7.0–16.3%), with long branches leading to each clade (posterior probabilities 1.00). The previously published sequence of *D. magna* falls within the NCNT clade, whereas the *D. bilineata* sequence lies outside of the *D. bilineata-D.magna* clade recovered in this analysis, suggesting this sequence may represent a misidentified specimen. Two samples that are highly divergent and appear to represent separate evolutionary lineages (NMVD73905 and NMVD73901) suggest that further sampling is needed in this region. Thus, these two samples were not included in further morphological and evolutionary comparative analyses.

There was no significant evidence of recombination in the sequenced nuclear dataset, as suggested by the *DualBrothers* graphical output (Suchard et al. 2003; Minin et al. 2005), therefore we proceeded with phylogenetic analysis. A subset of samples was selected from each of the clades recovered in the mitochondrial phylogeny, covering geographically widespread populations within the *D. magna–D. bilineata* monophyly. A total of 46 samples were sequenced for 1012 bp of the nuclear region RAG-1. An additional 12 species were also sequenced for RAG-1 (*A. muricatus*, *T. lineata* and 10 species of *Diporiphora*). Of the 1012 unambiguous sites, 75 were variable and 62 parsimony informative. The Bayesian analysis was performed using an evolutionary model in which each codon position in the RAG-1 gene had a separate partition, as this was strongly supported by Bayes factors (2 ln Bayes factors = 206; Appendix S2), and a 50% majority-rules tree was recovered (Appendix S8). The phylogenetic relationships recovered in analyses of the RAG-1 dataset are similar to those in the mtDNA, with long branches leading to each of the geographically isolated clades in most cases (Appendix S8). The monophyly of the mtDNA clades, are well supported in RAG-1, except for the NWQLD, NENT, and CA clades. The RAG-1 analyses confirm that the NK clade has a long history of isolation, whereas the most

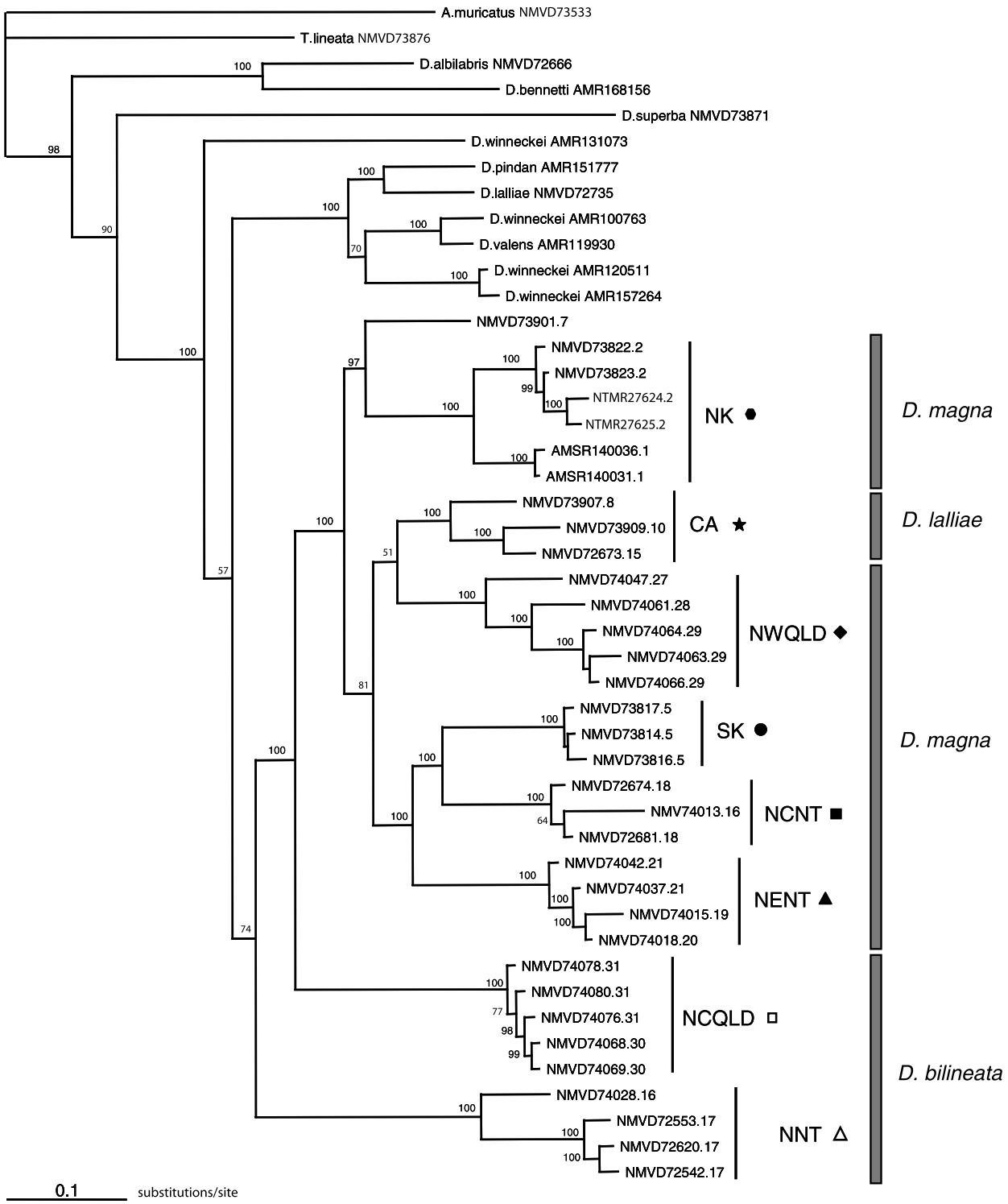

Figure 2. **A Bayesian 50% concensus phylogenetic tree of the combined analysis of ND2 and RAG-1 gene regions, with monophyletic clades labeled. Numbers adjacent to nodes indicate Bayesian posterior probabilities. Symbols indicate clades and correspond to Figures 3–5. Sample names represent museum voucher numbers, followed by the population number as shown in Figure 1.**

recently diverged clades (CA, SK, NCNT, NENT, NWQLD, NNT, NCQLD) comprise a large polytomy. Therefore, the sequence of cladogenesis for these clades remains unresolved with the nuclear dataset.

The PHT of the mtDNA and RAG-1 gene regions revealed the datasets were not significantly incongruent ($P = 0.21$). Thus, there was not a significant conflict between the two gene loci using a global test of combinability. As there was low heterogeneity

between each of the ND2 and RAG-1 datasets, along with the long, well-supported branches leading to each of the lineages, we considered a concatenated dataset represented the most accurate analysis for assessing species relationships. A partitioned Bayesian analysis was conducted on a concatenated dataset of the ND2 and RAG-1 regions (Fig. 2), using the evolutionary model strongly supported by Bayes factors, in which each gene had a separate partition (2 ln Bayes factors = 286–860; Appendix S2). The resulting 50% majority-rule consensus tree from this partitioned analysis is presented in Figure 2.

The topology of the combined tree has a similar structure to the separate mitochondrial and nuclear phylogenies and the eight clades recovered in the mtDNA analysis are again highly supported (posterior probabilities = 1.00). The levels of divergence between each of the clades recovered in both ND2 and RAG-1 are similar to previous fossil-calibrated studies on Australian agamid lizards, which date to the mid-late Miocene (Shoo et al. 2008; Melville et al. 2010a). Thus, this evidence suggests these represent deeply divergent and historically isolated lineages. Although there are a number of subclades observed within these clades, we chose to delimit the eight most divergent clades as taxonomic units. We used the method outlined in Wiens and Penkrot (2002) to initially diagnose the lineages, which incorporates haplotype and locality details to determine whether there is gene flow between lineages. We first examined the mitochondrial phylogeny, as this contained the largest dataset, then we compared clade position in RAG-1 and the concatenated analysis. However, we chose not to diagnose all of the 14 clades as distinct taxonomic units as would be suggested by this method. Instead, we used a conservative approach for diagnosing each of the clades because our geographic sampling is not continuous in some areas. Thus, geographic boundaries of clades were placed where further sampling would not result in the loss of a clade. For example, within the SK clade, the two individuals collected from population 13 form a separate lineage in the ND2 phylogeny, however, as no sampling has occurred in the region between population 13 and the other populations in this clade, we cannot assume that gene flow between these lineages does not occur. All eight diagnosed clades within the *D. magna-D. bilineata* group are allopatric, except for the NNT and NCNT clades, which overlap geographically with sympatric populations at Pine Creek but form highly divergent lineages (Fig. 1). These eight well-supported clades comprise three species, according to the current taxonomy: *D. bilineata* (NNT and NCQLD); *D. magna* (NWQLD, NK, NENT, SK, and NCNT); and *D. lalliae* (CA). Thus, the overall genetic evidence obtained from both nuclear and mitochondrial datasets supports the *D. magna-D. bilineata* complex as being composed of eight historically isolated lineages.

Table 1. Discriminant function analysis results showing how often individuals are correctly classified by lineage/species based on morphological data for (A) males and (B) females.

Morphological dataset	Cryptic lineages	Described species
A. Males		
Size, shape and meristic	75%	100%
Meristic only	75%	91.1%
B. Females		
Size, shape and meristic	86.5%	100%
Meristic only	75.7%	100%

DIFFERENCES AMONG CLADES IN MORPHOLOGY AND HABITAT USE

We used morphological data to test for the presence of cryptic species among each of the eight recovered phylogenetic lineages. Morphometric data are reported from 27 populations, representing individuals of all eight phylogenetic clades of the *D. bilineata-D. magna* complex (locality details provided in Appendix S3). We used discriminant function analysis to explore whether each of the eight cryptic lineages and the 10 described species of the *Diporiphora* genus could be identified by species based on phenotypic characters. When size and meristic characters are both included, the individuals within the cryptic clades could only be classified correctly by clade 75% of the time for males and 86.5% of the time for females (Table 1). In comparison, the closely related previously described species can be classified by species 100% of the time for both males and females. We believe this provides good evidence that the eight *D. bilineata, D. magna,* and *D. lalliae* lineages can be considered cryptic as these clades are incorrectly classified 13.5–25% of the time, compared with consistent correct identification in the previously described species.

We used PCA to visually and statistically explore whether there were significant differences in morphology and ecology among each of the phylogenetic lineages. For morphological measurements, mean PC scores for each phylogenetically inferred clade were plotted in multivariate space (Fig. 3; PC scores provided in Appendix S9). ANOVAs revealed significant differences between clades for both males (PC1: $F_{7,48} = 4.421$, $P < 0.001$; PC2: $F_{7,48} = 7.410$, $P < 0.001$) and females (PC1: $F_{7,27} = 5.095$, $P = 0.001$; PC2: $F_{7,27} = 2.560$, $P = 0.036$; PC3: $F_{7,27} = 5.364$, $P = 0.001$). A correspondence analysis was used to assess variation between phylogenetic clades in meristic characters. Initially, ANOVAs revealed significant differences between each of the phylogenetic clades (Fig. 4; CA scores provided in Appendix S10) for both males (F1: $F_{7,44} = 4.424$, $P = 0.001$; F2: $F_{7,44} = 4.755$, $P < 0.001$) and females (F1: $F_{7,28} = 14.442$, $P < 0.001$; F2: $F_{7,28} = 53.755$, $P = 0.005$). The singular and principal component

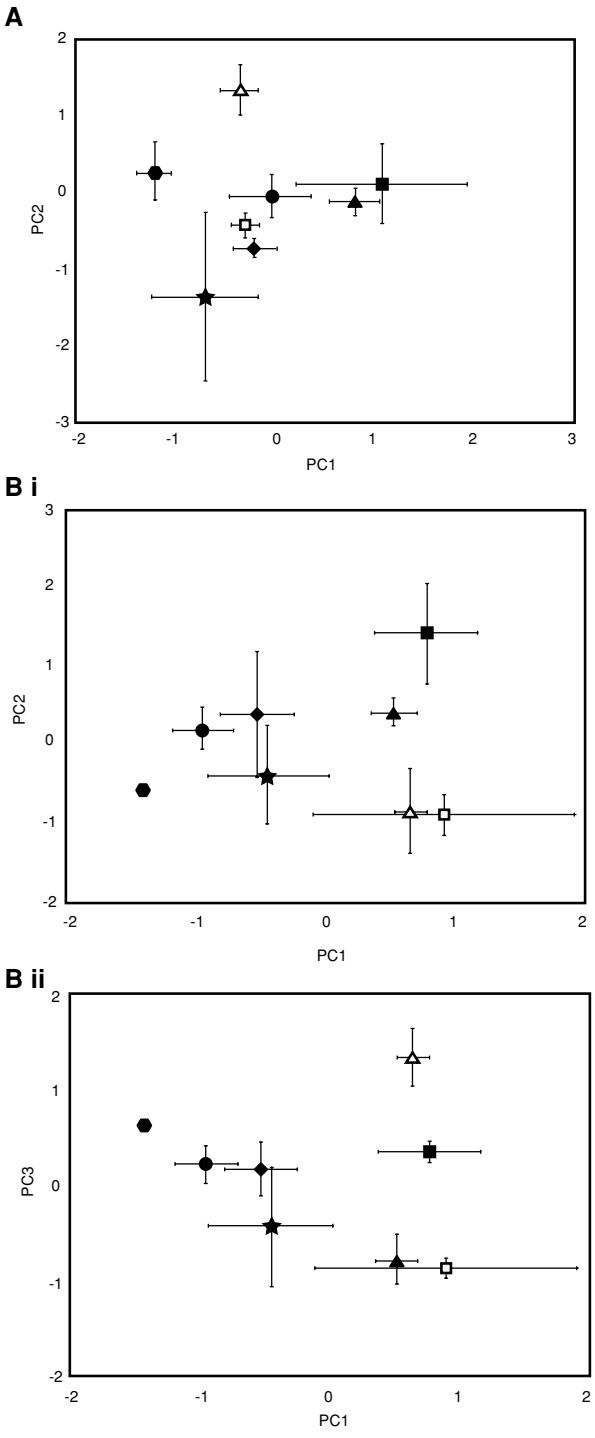

Figure 3. Ordination plots of mean PC scores for morphological measurements, with standard error bars, for each phylogenetic clade of the *D. bilineata–D. magna* complex (■ = NCNT, ⬣ = NNT, ▲ = NENT, • = SK, △ = NK, ♦ = NWQLD, □ = NCQLD, ⋆ = CA). Plots are presented for (A) males and (B i–ii) females.

scores from these analyses were subsequently used in hypothesis testing (see below). However, the central Australian clade (CA) displayed significant morphological divergence in meristic characters compared with all other clades, for both males and females

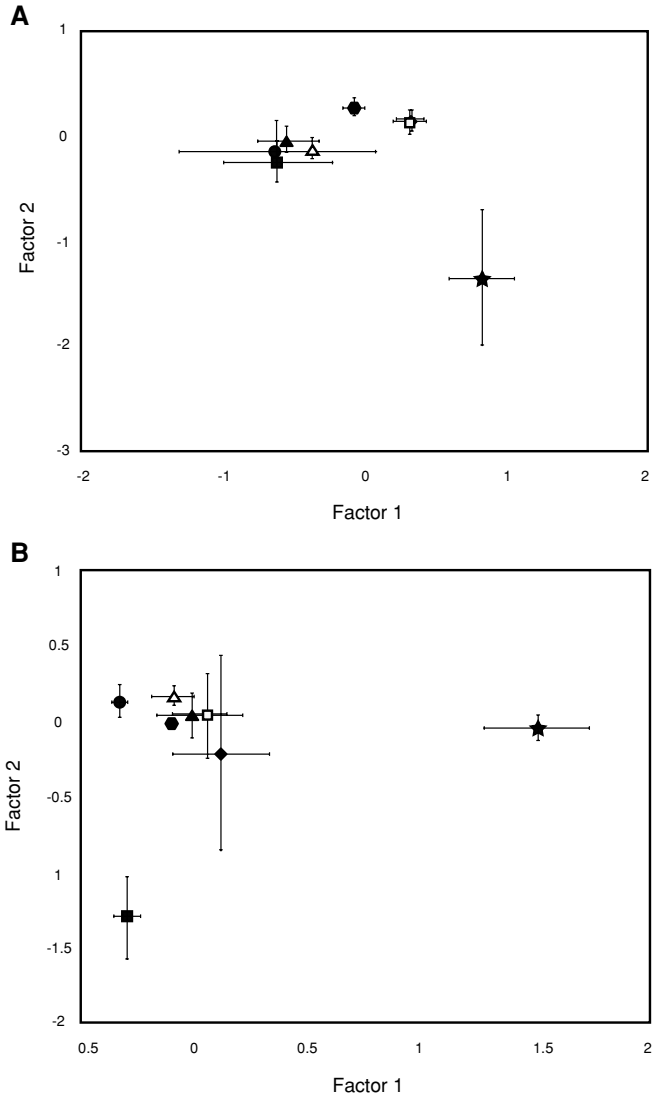

Figure 4. Ordination plots of mean meristic character scores, with standard error bars, for each clade of the *D. bilineata--D. magna* complex. Symbols correspond with the phylogenetic clade (■ = NCNT, ⬣ = NNT, ▲ = NENT, • = SK, △ = NK, ♦ = NWQLD, □ = NCQLD, ⋆ = CA). Plots are presented for (A) males and (B) females.

(see Appendix S11). This clade consists of individuals currently recognized as a distinct species (*D. lalliae*), based on the presence of a gular fold, a feature lacking in *D. bilineata* and *D. magna*. Consequently, we conducted the meristic character analyses excluding this clade to gain an understanding of the morphological divergence between the remaining clades (Fig. 5; CA scores provided in Appendix S12). No significant differences were found between clades for meristic characters in females (F1: $F_{6,25} = 1.763$, $P = 0.148$; F2: $F_{6,28} = 1.579$, $P = 0.195$), whereas five distinct clusters exist in males (F1: $F_{6,42} = 7.919$, $P < 0.001$; F2: $F_{6,42} = 9.554$ $P < 0.001$; Fig. 5). Although these clusters are distinct in multivariate space, the characters heavily weighted for each component and therefore deemed to be divergent between

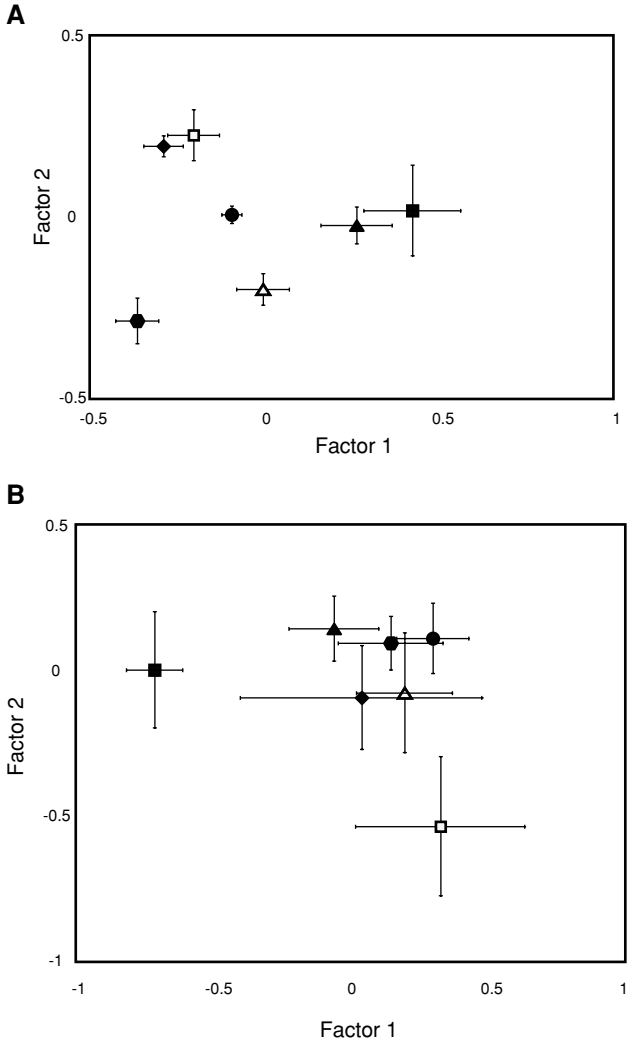

Figure 5. Ordination plots of mean morphology scores, with standard error bars, for each clade of the *D. bilineata* and *D. magna* complex, excluding the CA clade. Symbols correspond with phylogenetic clades (■ = NCNT, ⬣ = NNT, ▲ = NENT, • = SK, △ = NK, ♦ = NWQLD, □ = NCQLD, ★ = CA). Plots are presented for (A) males and (B) females.

clades from this analysis, do not represent characters that would be morphologically diagnostic in the field (e.g., strength of the nuchal crest, strength of body and tail patterning). Furthermore, the morphological characters found to be divergent between clades are not the same for both males and females. Therefore, as there has been very little apparent morphological divergence, despite the deep phylogenetic divergences, we consider these clades to be cryptic.

Ecological data are reported from 19 populations, representing 67 individuals (39 males, 28 females) from seven clades of the *D. bilineata-D. magna* complex (Appendices S13 and S14). Multivariate analysis of differences between clades in microhabitat variables (dependent on the behavior of the lizard) showed significant differences between clades for males on PC2 ($F_{4,31} = 5.443$, $P = 0.002$) and females on PC1 ($F_{3,18} = 4.358$, $P = 0.018$) and PC2 ($F_{3,19} = 7.998$, $P = 0.001$). However, there were no significant differences for males on PC1 ($F_{4,31} = 1.847$, $P = 0.145$) and for females on PC3 ($F_{3,19} = 1.745$, $P = 0.192$). Multivariate analysis of structural habitat variables (general ecological features within a 3 m radius) showed that some clades did differ significantly for males on PC2 ($F_{4,31} = 3.082$, $P = 0.030$) and PC3 ($F_{4,31} = 3.152$, $P = 0.028$) and for females on PC2 ($F_{3,18} = 5.921$, $P = 0.005$). However, clades did not differ significantly for males on PC1 ($F_{4,31} = 0.294$, $P = 0.879$) and for females on PC1 ($F_{3,18} = 1.140$, $P = 0.360$) and PC3 ($F_{3,18} = 2.947$, $P = 0.061$). Details of multivariate ecology analyses are reported in Appendix S15. Results for PCA of environmental data are reported in Appendix S16.

EVOLUTIONARY PROCESSES

Hypothesis 1: Phenotypic evolution fits a neutral model of Brownian motion

Blomberg's K statistic (Blomberg et al. 2003) showed significant phylogenetic structure for only one variable, female structural habitat ($P = 0.03$). This indicates that females that occupy similar structural habitats are phylogenetically related. All other morphological and ecological datasets did not show a significant relationship with phylogeny (all datasets: $P > 0.05$; Table 2). This indicates that there is no statistical support for phylogenetic structure in these datasets for nearly all variables and that as a result of evolutionary stasis, the phylogenetic divergence of lineages does not predict patterns of phenotypic divergence. Thus, these results suggest that historical signal has been overwritten by nonrandom processes in all phenotypic traits, except that of female structural habitat.

Table 2. Blomberg's K statistic and *P*-values testing for phylogenetic signal in the morphological and ecological datasets in (A) males and (B) females. *P*-values <0.05 indicate significant phylogenetic structure in that character (indicated by asterisk).

Morphological/ecological dataset	K	*P*
A. Males		
Size	0.78	0.23
Shape	1.22	0.29
Meristic	1.19	0.16
Microhabitat	0.90	0.10
Structural	1.17	0.11
B. Females		
Size	0.89	0.87
Shape	0.94	0.51
Meristic	0.99	0.41
Microhabitat	0.95	0.81
Structural	1.11	0.03*

Table 3. **AIC values comparing four models of evolution; Brownian motion (BM), Ornstein-Uhlenbeck (OU), white noise (WN), and early burst (EB), for each morphological and ecological dataset. Favored models for each variable are indicated by an asterisk (*=favored model, **=reasonable support).**

Morphological/ ecological dataset	BM	OU	WN	EB
A. Males				
Size	−6.52	−4.89	−6.87*	−4.52
Shape	19.61	21.03	19.04*	21.61
Meristic	15.98	17.74	15.79*	17.98
Microhabitat	13.45*	15.61	13.61	15.45
Structural habitat	10.93*	12.93	11.45	11.34
B. Females				
Size	−0.88	−0.90	−2.90**	1.12
Shape	24.88	25.69	23.69*	26.88
Meristic	18.21	19.00	17.00**	20.21
Microhabitat	14.37	14.72	12.72**	16.37
Structural habitat	16.10*	18.59	16.59	18.10

Hypothesis 2: Phenotypic evolution fits a model of constrained evolution

Likelihood model testing was used to assess support for the tempo and mode of phenotypic overlap in the *D. magna–D. bilineata* species complex. AIC values, comparing the goodness of fit of four models to the data, found somewhat contrasting results for morphological and ecological datasets (Table 3). In both males and females, body size, shape and meristic characters were best supported by a WN model of constant constraint, strongly suggestive of constrained evolution. Microhabitat occupation in females was also supported by a WN model. Support is higher for females than males, which reflects the patterns in the disparity-through-time plots (Fig. 6). In general, a number of the plots place the data close to the null expectation, such that all clades, regardless of their age, contain similar differences among clades. However, male size, shape, and meristic characters show a fluctuating pattern through time, leading to lower support in model testing. In contrast, for females, the pattern of morphological disparity through time shows a recent burst of disparity between the clades in body shape and size, meristic characters, and microhabitat occupation. These results indicate that females show a recent high level of average diversity among clades and now show substantial overlap with other clades in morphospace, providing higher support for the WN model. However, the "burst" of disparity near the present day is different from the expectation of a pure white-noise model, and may instead be caused by a burst of diversification in some relatively young clades. On the whole, phenotypic evolution through time is best supported by a model of constrained evolution.

Nearly all ecological datasets (male microhabitat, male structural habitat, and female structural habitat) were best supported by a Brownian motion model of evolution. This suggests that the evolution of habitat use is reasonably well-described by a Brownian motion model. This is reflected in the disparity-through-time plots that position the data either below or closely following the null expectation.

Hypothesis 3: Phenotypic evolution fits a model of correlated evolution

The results of the partial Mantel tests found that morphological distance was not significantly correlated with microhabitat occupation, structural ecology, or environment, following Bonferroni

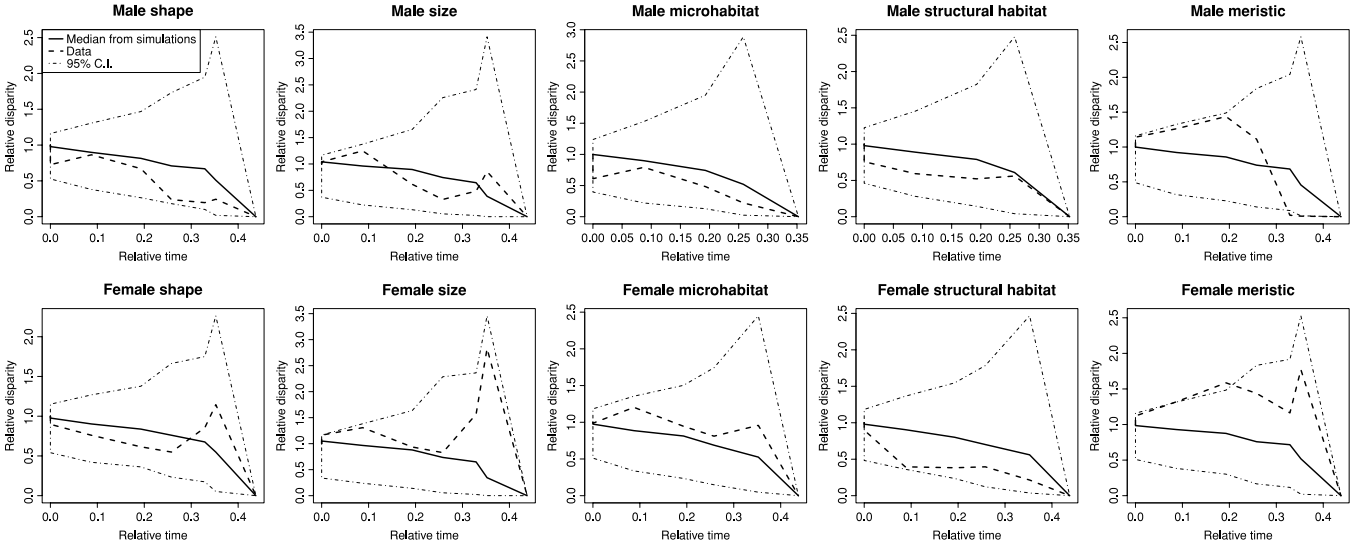

Figure 6. **Disparity-through-time plots calculated individually for each morphological and ecological dataset. The solid line indicates the relative disparity expectation according to a Brownian model of evolution; the dotted line is data from this study.**

sequential adjustments to estimate significance levels (Rice 1989; Appendix S17). These results imply that there is not an evolutionary correlation between ecology and morphology in the *D. magna-D. bilineata* species complex. Thus, this study found no evidence that the morphological differences between the clades of the complex result from adaptation to different habitats or environments occupied by the clades.

Discussion

Our study, which incorporates a combination of morphological, genetic, and ecological data, is the first to empirically test alternative hypotheses of evolutionary processes that may lead to morphological similarity among cryptic species. Our detailed analysis of morphology shows that in the *D. magna-D. bilineata* species group there are phylogenetic clades that show some morphological distinctness and others that could not be distinguished either with meristic characters or body shape analyses. Although multivariate analyses of morphological measurements and meristic characters revealed some significant differences, for the most part, the eight clades were not morphologically different and these patterns were not consistent between sexes. In females, morphology was highly variable, with no apparent phylogenetic or geographic pattern, whereas in males, groups of morphologically indistinguishable clades exist in both Queensland and the interior regions of the Northern Territory and Western Australia. In addition, closely related clades were not more similar morphologically. Thus, we believe that the combination of molecular and morphological data provides support that *D. bilineata* and *D. magna* species form a cryptic species complex.

The morphological stasis in the clades of *D. bilineata* and *D. magna,* combined with the high level of genetic divergences does not support neutral nonadaptive change as the primary cause of the morphological similarities for the majority of morphological characteristics examined. First, morphology in *D. bilineata* and *D. magna* clades did not show an association with phylogenetic distance, implying morphological divergence cannot be explained purely by neutral genetic change. The results from this analysis need to be treated with caution, as neutral genetic change can be present even if morphology and phylogenetic distance are not correlated. Therefore, additional evidence for processes other than neutrality was assessed using morphological disparity plots. These plots suggest a changing pattern of morphological evolution through time, strongly supported by a constrained model, which differs from Brownian model expectations. Thus, it is probable that a combination of nonadaptive evolution along with either correlated or constrained evolution underlies the cryptic speciation in the *D. bilineata* and *D. magna* species complex.

Correlated evolution, in which morphological evolution is driven by adaptation to novel ecological habitats, could have led to parallel evolution between the clades of *D. bilineata* and *D. magna* (Avise 2000). However, comparative evolutionary analyses, using partial Mantel tests, found no evidence of correlated evolution in the *D. bilineata* and *D. magna* species complex, as morphological variation was not correlated to either the habitat or environment occupied by evolutionary lineages. One caveat to these results is that, with eight clades, we have relatively low statistical power to resolve any correlations that might be present. Nonetheless, there are many causes of adaptive diversity (Losos and Miles 2002) and it is possible that a combination of ecological and environmental selection pressures, not covered in the current study, underlie morphological diversification in the *D. bilineata* and *D. magna* species complex.

We find the most compelling evidence that morphological diversity in *D. bilineata* and *D. magna* was shaped by constrained evolution, resulting in long-term morphological stasis in all the evolutionarily isolated lineages. An explanation for morphological stasis is not straightforward, as selective factors limiting morphological diversification are not easily distinguished from developmental constraints (Schlichting 1989) and an absence of fossil data means that it may not be clear whether a species has adapted over time (Losos and Glor 2003). Developmental constraints can act to constrain morphological evolution by putting restrictions on the ability of a species to morphologically evolve (Wake 1991). Although a detailed assessment of developmental constraints limiting morphological divergence is beyond the scope of this article, there is some evidence to suggest that more dramatic morphological change is theoretically possible in this species complex. For example, the morphologically divergent *D. lalliae* clade is phylogenetically placed within the complex, suggesting developmental constraints are not the only factor limiting morphological divergence of these cryptic lineages. Phylogenetic comparative analyses favored likelihood models with a constraint parameter (WN) for all phenotypic traits. This evidence, combined with the low levels of morphological differentiation in the *D. bilineata* and *D. magna* species complex over an extended period of time in geographic isolation, suggests that stabilizing selection may underlie the observed morphological stasis. Studies of cichlid fish have proposed that strong stabilizing selection has occurred in species occupying particular ecological niches whereas related species in alternative habitats diversified extensively (Sturmbauer and Meyer 1993). Similarly, a group of lizards closely related to *Diporiphora*, the genus *Ctenophorus*, show similar levels of sequence divergence between species (8–12%), but have high levels of morphological diversity, probably due to adaptation to a range of ecological and environmental conditions (Melville et al. 2001). Analysis of microhabitat occupation demonstrated that the clades of *D. magna* and *D. bilineata* occupy similar microhabitats with extensive ecological overlap between clades across the savannah woodlands of northern Australia (Appendix S15). Thus, the level

of spatial homogeneity in habitat and the similarity in ecological niche may be influencing evolution, leading to morphological stasis across the clades of *D. magna* and *D. bilineata* (Lecompete et al. 2005).

The tropical savannah woodlands of northern Australia are a temporally dynamic bioregion that fluctuates over different time scales; high fire regimes dramatically alter the vegetation on an annual basis (Russell-Smith et al. 1998), whereas the woodlands have undergone dramatic expansions and contractions over the last 10 million years (Markgraf et al. 1995). It has been argued that in dynamically changing environments, species may be able to track habitats faster than the rate at which they can adapt to new environmental conditions. In this case morphological stasis would result due to the inability of the species to adapt quickly enough (Wiens 2004; Kozak et al. 2006). Furthermore, it has also been proposed that these temporally fluctuating environments promote the evolution of stasis by selecting for long-term generalists that are relatively insensitive to environmental changes (Sheldon 1996). This pattern of stasis in fluctuating environments differs significantly from patterns found in the more temporally stable wet tropics, which are areas that are species rich (Crisp et al. 1995) and the high diversity of many endemic organisms has been attributed to greater opportunities for habitat specialization and diversification (Warheit et al. 1999). The high level of morphological stasis in the *D. magna* and *D. bilineata* species complex across the tropical savannahs of northern Australia favors a model of constrained morphological evolution. We suggest that the homogenous habitat structure combined with the fluctuating monsoonal climate provides a perpetually changing environment, which has promoted the evolution of morphological stability among clades of *D. magna* and *D. bilineata*.

In conclusion, this study has empirically quantified morphology in a cryptic species complex and examined specific mechanisms that could be responsible for conservatism over long periods of time accompanied by deep genetic divergences. The phenotypic differences between clades in the cryptic species, *D. bilineata* and *D. magna,* show an overriding signature of constrained evolution that we attribute to the temporally unstable environments across the savannah woodlands of northern Australia. However, these processes are probably moderated to a lesser extent by selection caused by climatic gradients and neutral change among some clades. Thus, the results from this study highlight the complexity of the relationship between genetic and phenotypic evolution, where multifarious evolutionary processes can lead to contemporary patterns in species diversity. The phenotypic and genetic patterns found in *D. magna* and *D. bilineata* are not likely to be restricted to *Diporiphora*, as many species of Australian agamids show patterns of extended isolation not accompanied by morphological change (e.g., Melville et al. 2010a,b). Therefore, rather than simply dismissing cryptic species as nonadaptive, we encourage continued cryptic species identification, followed by investigation of evolutionary processes, to allow a more advanced understanding of how morphological conservatism is maintained throughout widespread and historically isolated populations.

ACKNOWLEDGMENTS

We especially thank J. V. Buskirk for advice on project design and comments on drafts and analyses. We are grateful to D. Edwards, R. Koch, R. Glor, P. Horner, D. Horner, and W. Longmore for assistance with field work. We thank P. Doughty, R. Sadlier, and A. Amey for access to tissue samples, locality records and specimens. We are grateful to P. Horner, G. Shea, and R. Sadlier for advice on species identification, taxonomy and morphology. We thank D. Edwards, B. Ong, and A. Moussalli for advice on laboratory work and analyses, and S. Kembel and G. Hunt for providing computer code. Thanks to J. Wiens, J. Q. Richmond, D. C. Adams, C. C. Nice, J. Hale, members of the Harmon lab and three anonymous reviewers for comments on manuscript drafts. Funding was provided by an Australian Research Council Discovery Grant to JM.

LITERATURE CITED

Adams, D. C., C. M. Berns, K. H. Kozak, and J. J. Wiens. 2009. Are rates of species diversification correlated with rates of morphological evolution? Proc. R. Soc. Lond. B 276:2729–2738.

Akaike, H. 1974. A new look at the statistical model identification. IEEE Trans. Autom. Contr. 19:716–723.

Avise, J. C. 2000. Phylogeography: the history and formation of species. Harvard Univ. Press, Cambridge, MA.

Avise, J. C., J. Arnold, R. M. Ball, Jr., E. Bermingham, T. Lamb, J. E. Neigel, C. A. Reed, and N. C. Saunders. 1987. Intraspecific phylogeography: the mitochondrial DNA bridge between population genetics and systematics. Annu. Rev. Ecol. Evol. 18:489–522.

Bickel, R., and J. B. Losos. 2002. Patterns of morphological variation and correlates of habitat use in chameleons. Biol. J. Linn. Soc. 76:91–103.

Bickford, D., D. J. Lohman, N. S. Sodhi, P. K. L. Ng, R. Meier, K. Winker, K. K. Ingram, and I. Das. 2006. Cryptic species as a window on diversity and conservation. Trends Ecol. Evol. 22:148–155.

Blomberg, S. P., T. Garland Jr., and A. R. Ives. 2003. Testing for phylogenetic signal in comparative data: behavioral traits are more labile. Evolution 57:717–747.

Bostwick, K. S., and M. J. Brady. 2002. Phylogenetic analysis of wing feather taxis in birds: macroevolutionary patterns of genetic drift? The AUK 119:943–954.

Brandley, M. C., A. Schmitz, and T. W. Reeder. 2005. Partitioned Bayesian analyses, partition choice, and the phylogenetic relationships of scincid lizards. Syst. Biol. 54:373–390.

Bruna, E. M., R. N. Fisher, and T. J. Case. 1996. Morphological and genetic evolution appear decoupled in Pacific skinks (Squamata: Scincidae: Emoia). Proc. R. Soc. Lond. B. 263:681–688.

Burnham, K. P., and D. R. Anderson. 2002. Model selection and multimodel inference: a practical information-theoretical approach. 2nd ed. New York: Springer-Verlag.

Butler, M. A., and A. A. King. 2004. Phylogenetic comparative analysis: a modeling approach for adaptive evolution. Am. Nat. 164:683–695.

Castellano, S., and E. Balleto. 2002. Is the partial Mantel test inadequate? Evolution 56:1871–1873.

Charlesworth, B., R. Lande, and M. Slatkin. 1982. A neo-Darwinian commentary on macroevolution. Evolution 36:474–498.

Cogger, H. G. 2000. Reptiles and amphibians of Australia. 6th ed. Reed New Holland, Sydney, Australia.

Crisp, M. D., H. P. Linder, and P. H. Weston. 1995. Cladistic biogeography of plants in Australia and New Guinea: congruent pattern reveals two endemic tropical tracks. Syst. Biol. 44:457–473.

Drummond, A. J., B. Ashton, M. Cheung, J. Heled, M. Kearse, R. Moir, S. Stones-Havas, T. Thierer, and A. Wilson. 2009. Geneious v4.7. Available from http://www.geneious.com/

Edwards, S. V., L. Liu, and D. K. Pearl. 2007. High-resolution species trees without concatenation. Proc. Natl. Acad. Sci. USA 104:5936–5941.

Eldredge, N., and S. J. Gould. 1972. Punctuated equilibria: an alternative to phyletic gradualism. Pp. 82–115 *in* T. J. M. Schopf, ed. Models in paleobiology., Freeman Cooper, San Francisco.

Farris, J. S., M. Kallersjo, A. G. Kluge, and C. Bult. 1994. Testing significance of incongruence. Cladistics 10, 315–319.

Futuyma, D. J. 1998. Evolutionary biology. 3rd ed. Sinauer, Sunderland, MA.

Glor, R. E., J. J. Kolbe, R. Powell, A. Larson, and J. B. Losos. 2003. Phylogenetic analysis of ecological and morphological diversification in Hispaniolan trunk-ground anoles (*Anolis cybotes* group). Evolution 57:2383–2397.

Glor, R. E., M. E. Gifford, A. Larson, J. B. Losos, L. R. Schettino, A. R. C. Lara, and T. R. Jackman. 2004. Partial island submergence and speciation in an adaptive radiation: a multilocus analysis of the Cuban green anoles. Proc. R. Soc. Lond. B. 271:2257–2265.

Greer, A. E. 1989. The biology and evolution of Australian lizards. Surrey Beatty & Sons, Chipping Norton, NSW, Australia.

Hansen, T. F. 1997. Stabilizing selection and the comparative analysis of adaptation. Evolution 51:1341–1351.

Harmon, L. J., and R. E. Glor. 2010. Poor statistical performance of the Mantel test in phylogenetic comparative analyses. Evolution 64:2173–2178.

Harmon, L. J., J. A. Schulte, II, A. Larson, and J. B. Losos. 2003. Tempo and mode of evolutionary radiation in Iguanian lizards. Science 301:961–964.

Harmon, L. J., J. J. Kolbe, J. M. Cheverud, and J. B. Losos. 2005. Convergence and the multidimensional niche. Evolution 59:409–421.

Harmon, L. J., J. Weir, C. Brock, R. E. Glor, and W. Challenger. 2008. GEIGER: Investigating evolutionary radiations. Bioinformatics 24:129–131.

Harmon, L. J., J. B. Losos, J. Davies, R. G. Gillespie, J. L. Gittleman, W. B. Jennings, K. Kozak, M. A. McPeek, F. Moreno-Roark, T. J. Near, et al. 2010. Early bursts of body size and shape evolution are rare in comparative data. Evolution 64:2385–2396.

Harvey, P. H., and M. D. Pagel. 1991. The comparative method in evolutionary biology. Oxford Univ. Press, Oxford, NY.

Hunt, G. 2006. Fitting and comparing models of phyletic evolution: random walks and beyond. Paleobiology 32:578–602.

Kass, R. E., and A. E. Raftery. 1995. Bayes factors. J. Am. Stat. Assoc. 90:773–795.

Kearney, M. R., A. Moussalli, J. Strasburg, D. Lindenmayer, and C. Moritz. 2003. Geographic parthenogenesis in the Australian arid zone: I. A climatic analysis of the *Heteronotia binoei* complex (Gekkonidae). Evol. Ecol. Res. 5:953–976.

Kembell, S., D. Ackerly, S. Blomberg, P. Cowan, M. Helmus, H. Morlon, and C. Webb. 2009. Picante: R tools for integrating phylogenies and ecology. R package version 0.7-0. Available at http://www.CRAN.R-project.org/package=picante (accessed April 20, 2008).

Knowlton, N. 1993. Sibling species in the sea. Annu. Rev. Ecol. Evol. Syst. 24:189–216.

Kozak, K. H., A. Larson, R. M. Bonett, and L. J. Harmon. 2005. Phylogenetic analysis of ecomorphological divergence, community structure, and diversification rates in dusky salamanders (Plethodontidae: Desmognatus). Evolution 59:2000–2016.

Kozak, K. H., D. W. Weisrock, and A. Larson. 2006. Rapid lineage accumulation in a non-adaptive radiation: phylogenetic analysis of diversification rates in eastern North American woodland salamanders (Plethodontidae: Plethodon). Proc. R. Soc. Lond. B. 273:539–546.

Larson, A. 1989. The relationship between speciation and morphological evolution. Pp. 579–598 *in* D. Otte and J. A. Endler (Eds.), Speciation and its consequences. Sinauer Associates, Sunderland, MA.

Lecompte, E., C. Denys, and L. Granjon. 2005. Confrontation of morphological and molecular data: the *Praomys* group (Rodentia, Murinae) as a case of adaptive convergences and morphological stasis. Mol. Phylogenet. Evol. 37:899–919.

Lee, C. E. 2000. Global phylogeography of a cryptic copepod species complex and reproductive isolation between genetically proximate "populations". Evolution 54:2014–2027.

Legendre, P., and L. Legendre. 1998. Numerical ecology. Elsevier, Amsterdam, NL.

Lemos, B., G. Marroig, and R. Cerqueira. 2001. Evolutionary rates and stabilizing selection in large-bodied opossum skulls (Didelphimorphia: Didelphidae). J. Zool. 255:181–189.

Losos, J. B., and R. E. Glor. 2003. Phylogenetic comparative methods and the geography of speciation. Trends Ecol. Evol. 18:220–227.

Losos, J. B., and D. B. Miles. 2002. Testing the hypothesis that a clade has adaptively radiated: Iguanid lizard clades as a case study. Am. Nat. 160:147–157.

Losos, J. B., M. Butler, and T. W. Schoener. 2003. Sexual dimorphism in body size and shape in relation to habitat use among species of Caribbean *Anolis lizards*. Pp. 356–380 in S. F. Fox, J. K. McCoy and T. A. Baird, eds., Lizard social behavior. Johns Hopkins Press, Baltimore.

Lynch, M. 1990. The rate of morphological evolution from the standpoint of the neutral expectation. Am. Nat. 136:727–741.

Macey, J. R., A. Larson, N. B. Ananjeva, Z. L. Fang, and T. J. Papenfuss. 1997. Two novel gene orders and the role of light-strand replication in rearrangement of the vertebrate mitochondrial genome. Mol. Biol. Evol. 14:91–104.

Macey, J. R., J. A. Schulte, II, A. Larson, N. B. Ananjeva, Y. Wang, R. Pethiyagoda, N. Rastegar-Pouyani, and T. J. Papenfuss. 2000. Evaluating trans-tethys migration: an example using acrodont lizard phylogenetics. Syst. Biol. 49:233–256.

Mantel, N. 1967. The detection of disease clustering and a generalized regression approach. Cancer Res. 27:209–220.

Markgraf, V., M. McGlone, and G. Hope. 1995. Neogene paleoenvironmental and paleoclimatic change in southern temperate ecosystems: a southern perspective. Trends Ecol. Evol. 10:143–147.

Mathews, L. M., C. D. Schubart, J. E. Neigel, and D. L. Felder. 2002. Genetic, ecological, and behavioural divergence between two sibling snapping shrimp species (Crustacea: Decapoda: Alpheus). Mol. Ecol. 11:1427–1437.

Maynard Smith, J., R. Burian, S. Kauffman, P. Alberch, J. Campbell, B. Goodwin, R. Lande, D. Raup, and L. Wolpert. 1985. Developmental constraints and evolution. Q. Rev. Biol. 60:265–567.

McMahon, J. P., M. F. Hutchinson, H. A. Nix, and K. D. Ord. 1995. ANUCLIM User's Guide, Version 1. Centre for Resource and Environmental Studies, Australian National University, Canberra.

Melville, J., J. A. Schulte II, and A. Larson. 2001. A molecular phylogenetic study of ecological diversification in the Australian lizard genus *Ctenophorus*. J. Exp. Zool. Part B 291:339–353.

Melville, J., L. J. Harmon, and J. B. Losos. 2006. Intercontinental community convergence of ecology and morphology in desert lizards. Proc. R. Soc. Lond. B 273:557–563.

Melville, J., E. G. Richie, S. N. J. Chapple, R. E. Glor, and J. A. Schulte II. 2010a. Evolutionary origins and diversification of

dragon lizards in Australia's tropical savannas. Mol. Phyl. Evol., doi:10.1016/j.ympev.2010.11.025 [Epub ahead of print].

———. 2010b. Taxonomic revision of Australian agamid lizards from the genera *Amphibolurus* and *Lophognathus* (Lacertilia: Agamidae). Zootaxa. *In press*.

Milinkovitch, M. C. 1995. Molecular phylogeny of cetaceans prompts revision of morphological transformations. Trends Ecol. Evol. 10:328–334.

Minin, V. N., F. Fang, K. S. Dorman, and M. A. Suchard. 2005. Dual multiple change-point model leads to more accurate recombination detection. Bioformatics 21:3034–3042.

Nylander, J. A. A., F. Ronquist, J. P. Huelsenbeck, and J. L. Nieves-Aldrey. 2004. Bayesian phylogenetic analysis of combined data. Syst. Biol. 53:47–67.

Pfenninger, M., S. Staubach, C. Albrecht, B. Streit, and K. Schwenk. 2003. Ecological and morphological differentiation among cryptic evolutionary lineages in freshwater limpets of the nominal form-group *Ancylus fluviatilis* (O.F. Muller, 1774). Mol. Ecol. 12:2731–2745.

Posada, D., and K. A. Crandall. 1998. Modeltest: testing the model of DNA substitution. Bioinformatics 14:817–818.

Rambaut, A., and M. Charleston. 2000. Phylogenetic Tree Editor v1.0 alpha 10. http://evolve.zoo.ox.ac.uk/software/TreeEdit/main.html

Raufaste, N., and F. Rousset. 2001. Are partial Mantel tests adequate? Evolution 55:1703–1705.

Revell, L. J., and L. J. Harmon. 2008. Testing quantitative genetic hypotheses about the evolutionary rate matrix for continuous characters. Evol. Ecol. Res. 10:311–321.

Revell, L. J., L. J. Harmon, and D. C. Collar. 2008. Phylogenetic signal, evolutionary process, and rate. Syst. Biol. 57:591–601.

Rice, W. R. 1989. Analyzing tables of statistical tests. Evolution 43:223–225.

Ronquist, F., J. P. Huelsenbeck, and P. Van Der Mark. 2005. MrBayes version 3.1: Bayesian Analysis of Phylogeny: Florida State University: http://mrbayes.csit.fsu.edu.

Rosenberg, M. S. 2002. PASSaGE: pattern analysis, spatial statistics and geographic exergesis http://www.passagesoftware.net/.

Russell-Smith, J., P. G. Ryan, D. Klessa, G. Waight, and R. Harwood. 1998. Fire regimes and fire-sensitive vegetation of the sandstone Arnhem plateau, monsoonal northern Australia: application of a remotely-sensed fire. J. Appl. Ecol. 35:829–846.

Sanderson, M. J. 2002. Estimating absolute rates of molecular evolution and divergence times: a penalized likelihood approach. Mol. Biol. Evol. 19:101–109.

Schlichting, C. D. 1989. Phenotypic integration and environmental change. BioScience 39:460–464.

Schluter, D. 2000. The ecology of adaptive radiation. Oxford Univ. Press, Oxford, NY.

Schluter, D., and J. D. McPhail. 1993. Character displacement and replicate adaptive radiation. Trends Ecol. Evol. 8:197–200.

Schneider, C., and Moritz. 1999. Rainforest refugia and evolution in Australia's wet tropics. Proc. R. Soc. Lond. B 266:191–196.

Schulte, J. A., J. Melville, and A. Larson. 2003. Molecular phylogenetic evidence for ancient divergence of lizard taxa on either side of Wallace's Line. Proc. R. Soc. Lond. B. 270:597–603.

Schulte, J. A., J. B. Losos, F. B. Cruz, and H. Nunez. 2004. The relationship between morphology, escape behaviour and microhabitat occupation in the lizard clade *Liolaemus* (Iguanidae : Tropidurinae : Liolaemini). J. Evol. Biol. 17:408–420.

Sheldon, P. R. 1996. Plus ca change—a model for stasis and evolution in different environments. Paleogeogr. Paleoclimatol. Paleoecol. 127:209–227.

Shoo, L. P., Rose, R. Doughty, P., Austin, J. J., and Melville, J. 2008. Diversification patterns of pebble-mimic dragons are consistent with historical disruption of important habitat corridors in arid Australia. Mol. Phylogenet. Evol. 48:528–542.

Smouse, P. E., J. C. Long, and R. R. Sokal. 1986. Multiple regression and correlation extensions of the Mantel test of matrix correspondence. Syst. Zool. 35:627–632.

Storr, G. M. 1974. Agamid lizards of the genera Caimanops, Physignathus and Diporiphora in Western Australia and Northern Territory. Records of the Western Australia Museum 3:121–146.

Sturmbauer, C., and A. Meyer. 1993. Mitochondrial phylogeny of the endemic mouthrooding lineages of cichlid fishes from Lake Tanganyika in Eastern Africa. Mol. Biol. Evol. 10:751–768.

Suchard, M. A., R. E. Weiss, K. S. Dorman, and J. S. Sinsheimer. 2003. Inferring spatial phylogenetic variation along nucleotide sequences: a multiple change-point model. J. Am. Stat. Assoc. 98:427–437.

Swofford, D. L. 2000. PAUP*. Phylogenetic Analysis Using Parsimony (*and Other Methods), 4.0 edition. Sinauer Associates, Sunderland, MA.

Wainwright, P. C., and S. M. Reilly. 1994. Ecological morphology: integrative organismal biology. Univ. Chicago Press, Chicago, USA.

Wake, D. B. 1983. On the problem of stasis in organismal evolution. J. Theor. Biol. 101:211–224.

———. 1991. The result of natural selection, or evidence of design limitations? Am. Nat. 138:543–567.

Warheit, K. I., J. D. Forman, J. B. Losos, and D. B. Miles. 1999. Morphological diversification and adaptive radiation: a comparison of two diverse lizard clades. Evolution 53:1226–1234.

Wiens, J. J. 1998. Combining data sets with different phylogenetic histories. Syst. Biol. 47:568–581.

———. 2004. Speciation and ecology revisited: phylogenetic niche conservatism and the origin of species. Evolution 58:193–197.

Wiens, J. J., and C. H. Graham. 2005. Niche conservatism: integrating evolution, ecology and conservation biology. Annu. Rev. Ecol. Evol. Syst. 36:519–539.

Wiens, J. J., and T. L. Penkrot. 2002. Delimiting species based on DNA and morphological variation and discordant species limits in spiny lizards (Sceloporus). Syst. Biol. 51:69–91.

Wilson, S. K., and D. G. Knowles. 1988. Australia's reptiles: a photographic reference to the terrestrial reptiles of Australia. Collins, Sydney, Australia.

Woinarski, J. C. Z., A. Fisher, and D. Milne. 1999. Distribution patterns of vertebrates in relation to an extensive rainfall gradient and variation in soil texture in the tropical savannas of the Northern Territory, Australia. J. Trop. Ecol. 15:381–398.

Associate Editor: C. Nice

Supporting Information

The following supporting information is available for this article:

Appendix S1. Localities of sequenced specimens.
Appendix S2. Partitioning strategies used in Bayesian analysis for each of the datasets.
Appendix S3. Locality details for morphologically analyzed male (M) and female (F) specimens.
Appendix S4. An ANOVA of each body size measurement revealed males ($N = 56$) were significantly larger than females ($N = 37$) in SVL ($F_{1,90} = 14.084$, $P < 0.001$), tail length ($F_{1,90} = 16.867$, $P < 0.001$), head length ($F_{1,90} = 20.865$, $P < 0.001$), head width ($F_{1,90} = 14.772$, $P < 0.001$), hindlimb length ($F_{1,90} = 26.412$, $P < 0.001$), forelimb length ($F_{1,90} = 12.494$, $P = 0.001$), interlimb length ($F_{1,90} = 6.040$, $P = 0.016$), metatarsal length ($F_{1,90} = 14.868$, $P < 0.001$) and metacarpal length ($F_{1,90} = 6.717$, $P = 0.011$).
Appendix S5. Morphological Measurements.
Appendix S6. The ecological measurements taken in the field ($N = 71$) were: (1) Thermal Characteristics (°C): Body: Thermistor probe placed in the cloaca; Surface: Observed perch site; Air: Shaded air temperature; (2) Microhabitat Characteristics: (a) Perch: Description of type of perch (trunk/termite mound/stick/log); Diameter of perch (cm); Height of perch (cm); (b) Shelter (nearest to capture location): Description of type of shelter (rock/grass/trunk); Distance from capture location to shelter (cm); (c) Vegetation (nearest to capture location): Description of type of vegetation (grass woodland/shrub woodland); Distance from capture location to vegetation (cm); (3) Structural Characteristics: (a) Ground (vegetation <30 cm): Percentage cover (%); (b) Shrub (vegetation 30–100 cm): Percentage cover (%); Height of shrub nearest to capture location (cm); (c) Tree (vegetation >1.5 m): Percentage cover (%); Height of tree nearest to capture location (cm); (d) Substrate: Description of substrate type (red sandy soil/grey sandy soil); Gravel (% cover); Litter (% cover); Rocks of varying size classes (% cover): (A) <5 cm, (B) 5–20 cm, (C) 20–50 cm, (D) 50–100 cm, (E) >100 cm.
Appendix S7. Mitochondrial DNA phylogeny.
Appendix S8. Nuclear phylogeny.
Appendix S9. Principal component scores and eigenvalues resulting from PCA of morphological measurements.
Appendix S10. Factor scores and eigenvalues from correspondence analysis of meristic characters.
Appendix S11. Summary of meristic character correspondence analysis.
Appendix S12. Factor scores and eigenvalues from correspondence analysis of meristic characters, excluding the CA clade (*D. lalliae*).
Appendix S13. Results from principal component analyses of microhabitat variables, including factor scores, eigenvalues, and percent variance.
Appendix S14. Principal component scores for structural ecology variables including factor scores, eigenvalues, and percent variance.
Appendix S15. Details of ecological multivariate analyses.
Appendix S16. Principal component scores for environmental variables including factor scores, eigenvalues, and percent variance.
Appendix S17. Results of partial Mantel tests on individuals of *D. magna* and *D. bilineata,* which examine the correlation between two matrices while holding phylogenetic distance constant.

Supporting Information may be found in the online version of this article.